

Atomistic simulations of diffusion mechanisms in stoichiometric Ni₃Al

This article has been downloaded from IOPscience. Please scroll down to see the full text article.

2006 J. Phys.: Condens. Matter 18 1381

(<http://iopscience.iop.org/0953-8984/18/4/022>)

View [the table of contents for this issue](#), or go to the [journal homepage](#) for more

Download details:

IP Address: 129.252.86.83

The article was downloaded on 28/05/2010 at 08:52

Please note that [terms and conditions apply](#).

Atomistic simulations of diffusion mechanisms in stoichiometric Ni₃Al

Jinsong Duan

Department of Materials Science and Engineering, The University of Liverpool,
Liverpool L69 3GH, UK

and

Department of Chemistry, Carnegie Mellon University, Pittsburgh, PA 15213, USA

E-mail: chemcpu@yahoo.com

Received 18 September 2005, in final form 15 November 2005

Published 13 January 2006

Online at stacks.iop.org/JPhysCM/18/1381

Abstract

The first molecular dynamics (MD) simulation of diffusion mechanisms in ordered stoichiometric Ni₃Al with the Finnis–Sinclair interatomic potential is reported in this paper. Results show that Ni atoms mainly diffuse through Ni sublattices via the vacancy mechanism; Al atoms diffuse via both the antistructure bridge and the intrasublattice mechanism. Molecular statics (MS) simulations are carried out to estimate the migration energy barriers for the elementary jumps and the different diffusion mechanisms with both the ‘embedded atom method’ and Finnis–Sinclair interatomic potentials. It is proven that the six-jump cycle mechanism is not energetically favourable because of the high migration energy. Thus, MD and MS simulations yield the same results on the diffusion mechanism in stoichiometric Ni₃Al. Ni diffusion mechanisms obtained in this work agree with experimental results and theoretical calculation.

(Some figures in this article are in colour only in the electronic version)

1. Introduction

The nickel aluminide alloy Ni₃Al has been the subject of extensive experimental studies and theoretical modelling [1–3] because of its wide range of applications in high temperature components working in harsh environments—high temperature and corrosion. For example, this aluminide can be used as a furnace component, resistance heating element and component for gas, water and steam turbines. The failure mechanisms for these components such as creep, which is the diffusion-controlled process, have not been fully understood. Thus, investigations of diffusion mechanisms are of interest for both practical and scientific reasons.

Ni₃Al has the L1₂ structure, as illustrated in figure 1. Ni atoms occupy the six face centres, constituting Ni sublattices, and Al atoms occupy the eight corners, constituting Al sublattices. There are three Ni sublattices and one Al sublattice in the unit cell of Ni₃Al.

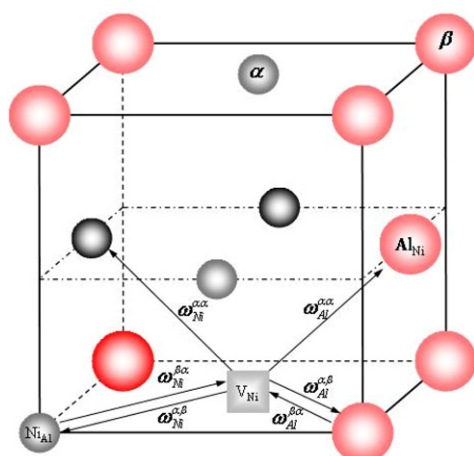


Figure 1. The unit cell of Ni_3Al . Ni atoms occupy Ni sublattices (denoted as α), Al atoms occupy Al sublattices (denoted as β). $\omega_{\text{Ni}}^{\alpha\alpha}$ is the jump of a Ni atom from one α sublattice site to another α sublattice site. $\omega_{\text{Ni}}^{\alpha\beta}$ is the jump of a Ni atom from an α sublattice site to a β sublattice site. $\omega_{\text{Ni}}^{\beta\alpha}$ is the jump of a Ni atom from a β sublattice site to an α sublattice site. The notes for Al atoms have analogous meanings.

Both experimental studies [4, 5] and thermodynamics calculation [6] indicate that there are two types of defects—vacancies and antisite defects in ‘stoichiometric’ Ni_3Al or $\text{Ni}_{75}\text{Al}_{25}$ where there are three Ni atoms and one Al atom in the unit cell of Ni_3Al . In particular, defects are the Ni vacancy (V_{Ni}), Al vacancy (V_{Al}), Ni antisite (an Al atom on a Ni lattice site, Al_{Ni}), and Al antisite (a Ni atom on an Al lattice site, Ni_{Al}). The definitions of the above point defects are identical to those in [7, 8]. They are thermal defects. The diffusion process in Ni_3Al at elevated temperature ($T > 1250$ K) is controlled by Ni vacancies. The thermodynamics calculation [6] showed that at 1500 K the Ni vacancy concentration is 1.0×10^{-5} at.%, the Al vacancy concentration is 5.6×10^{-7} at.%, and the concentration of Ni antisites and Al antisites is equal, that is 1.0×10^{-3} at.%. Our simulations are just based on the fact that Ni vacancies dominate diffusion in this particular composition of Ni_3Al .

The radiotracer experiment studies (using radioactive ^{63}Ni) of Ni diffusion in Ni_3Al are illustrated in figure 2. As shown in figure 2, at high temperatures ($T > 1250$ K) the Ni self-diffusion coefficients obtained by different researchers [4, 9, 10], with the exception of Larikov [11], are in good agreement and can be fitted into a single Arrhenius plot.

From the above experiments, the activation energy (E) for Ni atom migration is estimated to be 3.03 eV and the diffusion coefficient (D_{Ni}^*) is estimated to be $3.59 \times 10^{-4} \text{ m}^2 \text{ s}^{-1}$. The activation energy value is in agreement with the summation of the formation energy (1.6 ± 0.2 eV) and the migration energy (1.2 ± 0.2 eV) for the Ni vacancy in Ni_3Al (values estimated in [12] from a positron annihilation experiment). Therefore, Ni diffusion in Ni_3Al is expected to occur via the vacancy migration through Ni sublattices.

The radioactive ^{26}Al isotope is so unstable that it is difficult to carry out any radiotracer experiment of Al diffusion in Ni_3Al . The only radiotracer experiment results of Al diffusion by Larikov [11], as illustrated in figure 3, are doubtful because the Ni self-diffusion data reported in the same experiment are of higher magnitude than these obtained by other researchers (see figure 2).

However, some other tracer atoms (foreign atoms such as In, Ga, Ge, Ti and Nb) can replace the radioisotope ^{26}Al in impurity diffusion experiments [10, 13] if they are located

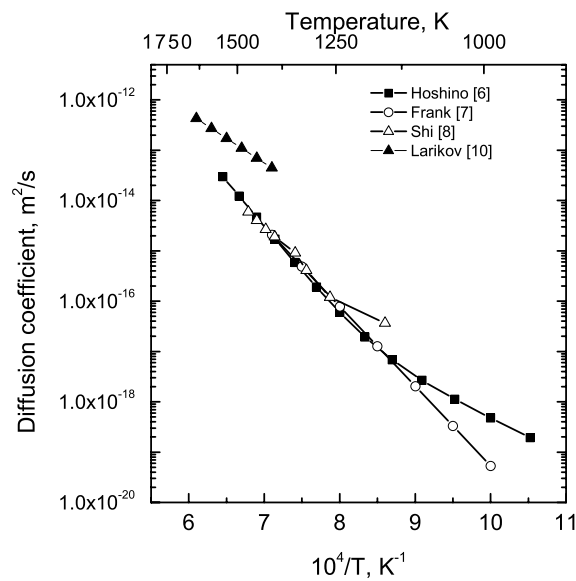


Figure 2. The temperature dependence of the diffusion coefficient of Ni in Ni₃Al by different researchers.

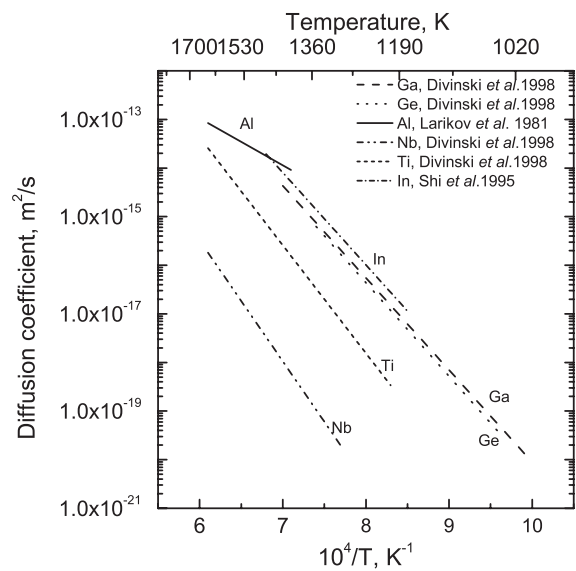


Figure 3. The temperature dependence of the diffusion coefficient of Al and Al substituting elements in Ni₃Al.

on Al sublattices in Ni₃Al. The results are shown in figure 3. It can be seen that there are big differences between the diffusion coefficients of such Al-substituting elements. These differences have been interpreted in terms of the different diffusion mechanisms operating (mainly the intrasublattice and antistructure bridge mechanisms). However, Koiwa [14] argued that it is not obviously valid to match the diffusion coefficients of foreign atoms to these mechanisms of Al in Ni₃Al.

Ikeda *et al* [15] calculate the Al self-diffusion coefficient by fitting the interdiffusion data of Ni₃Al into the Darken–Manning model [16]. At 1400 K, the Al self-diffusion coefficient was estimated to be smaller by a factor of three to four than that of Ni self-diffusion. The composition dependence of D_{Al} was also examined. D_{Al} increases with Al composition, which is consistent with the diffusion mechanism that Al diffuses through the Ni sublattice as an impurity [14]. Ikeda *et al* [15] study diffusion in Ni₃AlNi₃Ga and Ni₃Ge, and show in the experiment that the Darken–Manning model is valid for Ni₃Ga. Belova *et al* [17] proves theoretically that the Darken–Manning equation is also valid in the case of Ni₃Al. Fujiwara *et al* [18] demonstrate that Ni and Al atoms have similar diffusion rates. So far, no clear conclusions on Al diffusion mechanisms have been obtained from experimental studies.

In summary, the experimental investigations yield the following conclusions on the diffusion mechanisms in Ni₃Al.

- (1) Ni atoms diffuse through Ni sublattices via the vacancy mechanism.
- (2) The Al atom diffusion mechanisms are largely unknown.

Apart from experimental investigations, some theoretical works have been done on diffusion in Ni₃Al. There are several theoretical models proposed for the diffusion mechanisms in ordered alloys A₃B having the L1₂ structure. These models (the general vacancy mechanism, the intrasublattice mechanism, the antistructure bridge mechanism, and the six-jump cycle mechanism) are applied to Ni₃Al. Ni₃Al can keep the ordered structure up to the melting point [1]. Therefore, all theoretical models are designed to explain the diffusion mechanisms in crystals that would allow diffusion to occur with the ordered crystal structure remaining.

As mentioned above, diffusion in Ni₃Al is predominated by the Ni vacancy. Thus, we review here the general vacancy mechanism model. Other models will be discussed together with molecular dynamics simulation results in section 3.

The general vacancy mechanism model was proposed by Bakker and Westerveld [19]. To simplify, it is assumed that the vacancy jump frequency is only lattice dependent and the compound is in the state of thermal equilibrium order. Diffusion coefficients in a number of cubic ordered binary compounds can be derived on the basis of these assumptions. Debiaggi [20] applied this model to Ni₃Al, and proposed the following Ni diffusion coefficient:

$$D_{\text{Ni}}^* = D_0^{\text{NiNi}} \exp(-E^{\text{NiNi}}/\kappa_{\text{B}}T) + D_0^{\text{NiAl}} \exp(-E^{\text{NiAl}}/\kappa_{\text{B}}T), \quad (1)$$

where D_0^{NiNi} and D_0^{NiAl} are constants and E^{NiNi} and E^{NiAl} are the activation energies for Ni atoms. In equation (1), the first term is concerned with the intrasublattice jump ($\alpha \leftrightarrow \alpha$); the second term is related to the intersublattice jump ($\alpha \leftrightarrow \beta$), including the disordering jump ($\omega_{\text{Ni}}^{\alpha\beta}$) and the re-ordering jump ($\omega_{\text{Ni}}^{\beta\alpha}$) (see figure 1). At thermodynamic equilibrium, the jump frequencies of the disordering jump and the ordering jump are equal and the degree of order of Ni₃Al will not change with time.

The development of supercomputers makes it possible to simulate a time-consuming physical process such as diffusion dynamics. The often-used methods are molecular dynamics (MD), molecular statics (MS) and Monte Carlo (MC). Debiaggi [20] simulated Ni diffusion in Ni₃Al with the Bakker and Westerveld model [19] using MC modelling. The results show that simple vacancy–Ni atom interchange jumps are energetically favourable in comparison with the six-jump cycle mechanism.

To carry out kinetic Monte Carlo (KMC) simulations, the diffusion data should be available from experiments or MD simulations to parametrize the atomistic kinetic model in such a simulation. Athenes [21] investigated diffusion in A₃B of the L1₂ structure by means of KMC, where diffusion coefficients of A and B are set to be of the same order of magnitude. However,

it is difficult to apply KMC in the case of Ni₃Al to get reliable results because of the lack of Al diffusion data (either experimentally or theoretically).

All the above statements have led me to undertake simulation of diffusion in Ni₃Al using both MD and MS simulations. These simulations, with the insight gained on the different types of jumps of Ni and Al atoms between the lattice sites, will enable me to identify which mechanisms are predominantly responsible for diffusion in Ni₃Al. The initial results from this study were published in [22]. The outline of the present paper is as follows. The methodologies are presented in section 2. The results are discussed in section 3. The conclusions are summarized in section 4.

2. Methodologies

Both MS and MD simulations are applied in this work. To carry out molecular simulation, the suitable interatomic potentials are required. Thus, the interatomic potentials applied in this work are reviewed first, followed by discussions of simulation methods.

2.1. Interatomic potentials

There are two main classes of n -body central potentials based on either the ‘embedded-atom method’ (EAM) of Daw and Baskes [23] or the method of Finnis and Sinclair [24] (FS). Foiles [25] and Vitek [26] parametrized the Ni–Al system using the EAM and the FS model, respectively. Gao and Bacon [7, 8] modified Vitek’s [26] interatomic potential and calculated the formation energies of point defects in Ni₃Al. The results were compared with those obtained by Caro [27] using the EAM interatomic potential. In the present study, both Foiles [25] and the modified FS type interatomic potential [7, 8] are applied in MS simulation. The modified FS type interatomic potential [7, 8] is applied in the MD simulations. The melting temperature (T_m) of Ni₃Al using this interatomic potential is determined to be 1650 K, close to the experimental value of 1668 K [1]. The other works using this modified FS type interatomic potentials are references [28–31].

2.2. Molecular dynamics simulation

The simplest diffusion occurs when an atom exchanges with a vacancy on one of its nearest neighbour sites. Each jump is called the elementary jump. The possible elementary jumps of Ni and Al in Ni₃Al are illustrated in figure 1.

In order to simulate the above six elementary jumps and other possible jumps which may not be known thus far (i.e., the intrasublattice jump of Al atoms between $\omega_{Al}^{\beta\beta}$), and calculate the diffusion coefficients for both Ni and Al atoms in Ni₃Al, the MD code must be modified in the following way.

- (1) *Identification of vacancies and antisite defects in Ni₃Al.* The lattice parameter applied is that of equilibrium at the temperature of simulation, i.e. 1300–1550 K. The lattice is subdivided into ‘Wigner–Seitz’ cells with their centres at the thermal equilibrium lattice sites. As a result, defects, vacancies and antisites can be defined in the following way. A cell with only one atom in it, and the atom on its home lattice site, is counted as a normal cell; if an atom is on a different sublattice, this cell is occupied by an antisite defect; a cell with no atom in it is a Ni or Al vacancy, according to the lattice site.
- (2) *Classification of diffusion mechanisms.* After a long enough simulation time, a large number of jumps of defects are collected. By analysing the configurations of jumps of each atomic species (Ni and Al), the diffusion mechanisms can be revealed. For instance,

the intrasublattice mechanism includes jumps of the same atom between sites of the same sublattices. The antistructure bridge mechanism consists of two successive intersublattice jumps. The details will be discussed in section 3.

- (3) *Calculation of the diffusion coefficient and correlation factor.* Manning [32] defined the diffusion coefficient for each atomic species (D_i^*) in a multi-component system and the Einstein equation is applied to each of them directly without considering the specific diffusion mechanism,

$$D_i^* = \langle \vec{R}_i^2 \rangle / 6t \quad (2)$$

where $\langle \vec{R}_i^2 \rangle$ is the mean square displacement for atomic species i and t is the diffusion time. As mentioned before, one Ni vacancy is introduced in the simulations. Therefore, the diffusion coefficient referred to hereafter is the diffusion coefficient per unit vacancy.

To find a correct vacancy diffusion coefficient by the MD simulation, one can use the method of trajectory decomposition [33]. The idea is to decompose a single long trajectory of the vacancy into a sequence of short independent trajectory segments by duration δT . Therefore, the individual diffusion coefficient of each segment is calculated over δT . The vacancy diffusion coefficient is averaged over all individual diffusion coefficients. Once the vacancy diffusivity D_i^v is determined the tracer correlation factor for atomic species i is given as

$$f_i = D_i^* / D_i^v. \quad (3)$$

It should be noted that the correlation factor estimated using equation (3) is the average correlation factor for the different mechanisms. Also, it is derived originally for the random alloys. The validity of this equation is acceptable with caution in the case of Ni diffusion, where Ni atoms diffuse mainly through the Ni sublattice.

2.3. Molecular statics simulation

Migration energies for the vacancy have been obtained by a simple energy minimization technique in a molecular statics simulation. The details of this method are presented in [34]. The following is a brief summary. One atom is moved along the diffusion path by a series of small displacements, each displacement being followed by an energy minimization of the total energy of the simulation block with respect to displacements of all other atoms. During the minimization, the jumping atom itself is also allowed to move around in the plane perpendicular to the displacement direction. The migration energy is defined as the difference in energy between the maximum energy configuration and the initial configuration. Using this method, the energy barrier for an elementary jump or diffusion mechanisms containing several elementary jumps can be estimated.

An elementary jump or a diffusion mechanism is studied in the light of its migration energy. The larger the migration energy is, the lower will be the probability of the mechanism.

2.4. Computer simulation conditions

A simulation block is cubic in shape and has $10 \times 10 \times 10$ unit cells, that is 4000 atoms. The periodic boundary condition is applied. All MS simulations are performed at zero temperature; the simulation block with one vacancy is fully relaxed before starting the simulation. (As mentioned before, Ni vacancies predominate and play an active role in diffusion in Ni_3Al ; moreover, the system is going to reach the equilibrium state in the MD simulation; the initial configuration is not that important. We do not introduce antisites (either Ni_{Al} or Al_{Ni}) for the time being, because they can be created, and reach a thermal equilibrium concentration

when the MD simulation is progressing; see section 3.1.2.) Thus, the simulated vacancy concentration (which approximates well to the vacancy concentration of 10^{-4} at.% at 1400 K, but deviates from the values at other temperatures—it should be pointed out that the actual number of vacancies has no meaning affecting the diffusion mechanism, which is of primary interest in the study) in the Ni sublattice site is increased artificially to its thermal equilibrium volume (i.e., the lattice parameter is increased from 3.567 Å at 0 K to 3.687 Å at 1550 K), corresponding to simulation temperatures in the range of 1400–1550 K with intervals of 50 K and an additional one at 1300 K, relaxed and then heated up to that temperature. The total pressure on the crystal is zero. The constant-pressure MD simulations are conducted in the microcanonical ensemble using the constraint methods [35, 36]. The MD simulations are carried out with 1 ns of equilibration, followed by a reasonably long trajectory from which averages are computed. The simulation time depends on the simulation temperature and jump frequencies of defects, but usually takes more than 30 ns with the timestep of 0.8 fs to simulate 3000 vacancy jumps at 1400 K, for example. The trajectories are integrated with the predictor–corrector algorithm.

3. Results and discussion

3.1. Molecular dynamics simulation of diffusion in Ni₃Al

3.1.1. Ni diffusion mechanisms in Ni₃Al. Study of the diffusion mechanisms in Ni₃Al is of the most interest in this simulation. We are interested in those jumps which do contribute to diffusion in Ni₃Al. The intrasublattice jump is the simplest one. The intersublattice jumps could form complicated configurations, such as the six-jump cycle mechanism; the antistructure bridge mechanism or others may not yet be known. Obviously, the ordering and disordering jumps are also included in the intersublattice jumps. After we fully analyse the elementary jumps, we sort out the jump configurations that appear repeatedly, and can be taken as mechanisms. As a result, we obtain the proportions of different types of jumps, such as the intrasublattice (Intra.) and antistructure bridge (ASB) jumps of both Ni and Al atoms. The data are calculated as follows. The second column is the percentage of Ni atom jumps as of the total atomic jumps. The third and fourth columns show the intrasublattice jumps and antistructure bridge jumps as percentages of the number of total Ni atom jumps, respectively. Since the summation of the numbers of Ni atom and Al atom jumps is the total number of atomic jumps, the percentages of Al atom jumps are not listed. The data for Al atoms (listed in table 1) have analogous meaning. Here we should emphasize that the intrasublattice jump for Al only refers to an Al atom jump on the Ni sublattice, $\omega_{\text{Ni}}^{\alpha\alpha}$; see section 3.1.2 for details.

It can be seen from table 1 that the self-diffusion process in Ni₃Al is dominated by diffusion of Ni atoms in the whole temperature ranges simulated. The number of Ni atom jumps accounts for around 90% of the total number of atomic jumps, as seen in table 1. From a crystallographic point of view, Ni sites form a three-dimensional penetrating sublattice; see figure 1. Thus, diffusion of Ni atoms can be treated as self-diffusion in a monatomic crystal by the vacancy mechanism. Table 1 shows that about 90% of Ni atoms migrate via the Ni vacancy. This is known as the intrasublattice jump. Thus, the order of Ni₃Al is unchanged.

Besides the intrasublattice jump, Ni atoms can jump between different sublattices by the intersublattice jump. If these two jumps occur successively in such a way that two Ni atoms migrate via an Al vacancy, as illustrated in figure 4, then this is termed as the antistructure bridge jump. In this case, a vacancy and antisite belong to different sublattices and are initially nearest neighbour. The Ni vacancy first exchanges with a Ni_{Al}, and then with a regular atom on the Ni sublattice. This process includes displacements of two Ni atoms.

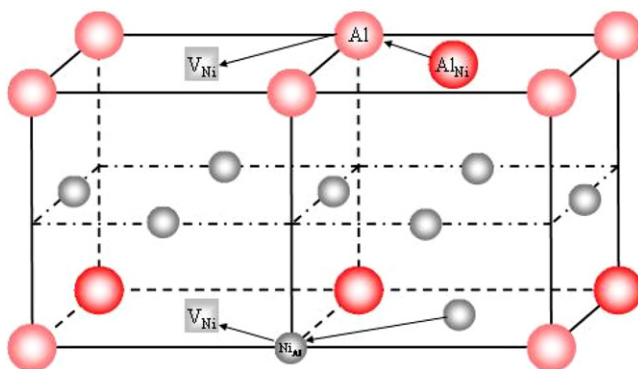


Figure 4. A scheme of the atomic arrangements according to the antistructure bridge mechanism in Ni_3Al . At the top is the ASB jump for Al atoms. The vacancy first exchanges with a regular atom on the Al sublattice and then with an antisite as follows: $V_{\text{Ni}} + \text{Al} \rightarrow \text{Al}_{\text{Ni}} + V_{\text{Al}}$, $V_{\text{Al}} + \text{Al}_{\text{Ni}} \rightarrow V_{\text{Ni}} + \text{Al}$; these exchanges include displacements of two Al atoms. The extra antisite Al_{Ni} created by the first jump is eliminated by the second jump, so that the initial order is restored. At the bottom is the ASB jump for Ni atoms, having analogous meaning.

Table 1. Percentage of Ni and Al atom jumps in Ni_3Al .

Temp. (K)	Ni			Al	
	Tot. Ni (%)	Intra. (%)	ASB (%)	Intra. (%)	ASB (%)
1550	86	87	1.0	31	19
1500	87	90	0.6	28	21
1450	90	90	0.9	19	27
1400	94	93	0.6	18	—
1300	94	91	0.5	10	—

This process can always be interrupted or even aborted, when the vacancy jumps away from the nearest neighbouring sites of Ni_{Al} . The antistructure bridge jump accounts for less than 1% of the total number of Ni atom jumps, as listed in table 1.

The above analysis indicates that the intrasublattice and antistructure bridge jumps promote Ni atom diffusion processes in which the Ni vacancy plays an important role.

3.1.2. Al diffusion mechanisms in Ni_3Al . The number of Al jumps accounts for no more than 15% of the total atomic jumps at the highest temperature considered and decreases to 6% at 1400 K, according to table 1. This suggests that at low temperature the diffusion of Al atoms is suppressed.

An Al site is entirely surrounded by 12 Ni sites, so as shown in figure 1 an Al atom jumps onto one of 12 nearest neighbour vacant sites, creating an antisite, $\omega_{\text{Al}}^{\beta\alpha}$. The Al vacancy created in this step can be occupied by a Ni atom jumping from a Ni site, $\omega_{\text{Ni}}^{\alpha\beta}$. As a result, a pair of Ni and Al antisites on nearest neighbour sites is created. This pair of antisites can be annihilated by the ordering jumps, such as $\omega_{\text{Ni}}^{\beta\alpha}$ and $\omega_{\text{Al}}^{\alpha\beta}$. After running the simulation for a long enough time, i.e., 15 ns, equal numbers of Ni and Al antisites are created, and the jump frequencies of the disordering jump and the ordering jump are equal. The concentrations of antisites created during the simulation reach a dynamic equilibrium, and do not change with time as shown in figure 6. If a disordering jump and an ordering jump occur in such a way that two Al atoms

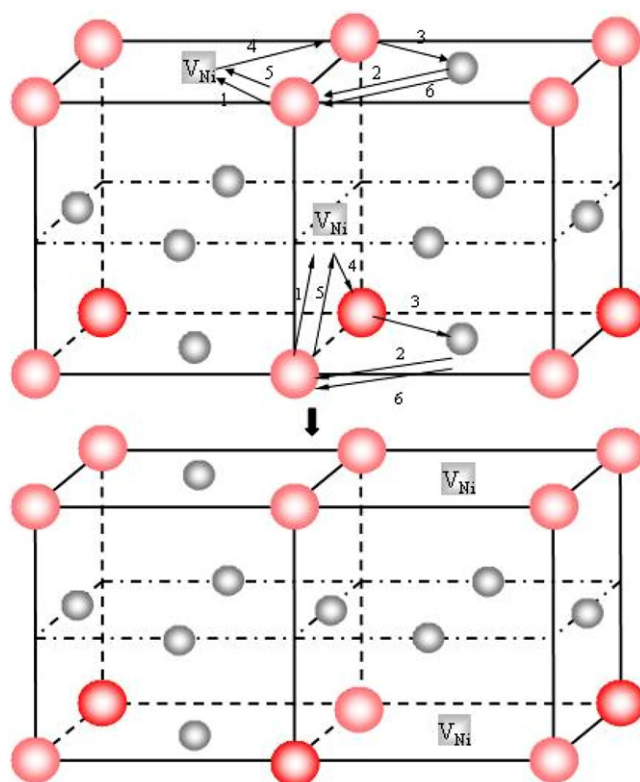


Figure 5. Six-jump cycle mechanism (at the top is a straight circle; at the bottom is a bent circle).

migrate successively, as illustrated in figure 4, then these two jumps are called the antistructure bridge jump of Al atoms by Divinski [13]. However, only a small number of jumps (20%–27%) among the total atomic jumps are antistructure bridge jumps.

It is suggested that the antistructure bridge jump can enhance Al diffusion by increasing the number of possible positions of Ni antisites that can be reached by a Ni vacancy after the first antistructure bridge jump [13]. This is true to some extent, but the frequency of a complete antistructure bridge jump is proportional to the concentration of Ni antisites and Ni vacancies. The equilibrium concentration of Al_{Ni} is 1.0×10^{-3} at.% at 1500 K [6]. It is predictable that Al diffusion is not significant.

Another Al_{Ni} concentration dependent migration proposed by Koiwa [14] is the intrasublattice jump in which an Al_{Ni} migrates through the Ni sublattice (see $\omega_{\text{Al}}^{\alpha\alpha}$ in figure 1). This type of jump accounts for more than 10% of the total Al jumps. This type of jump does not change the degree of order of the crystal. Both the antistructure bridge jump and intrasublattice jump make a comparable contribution to Al diffusion (see table 1). Since both mechanisms are Ni antisite concentration dependent, and Ni₃Al is highly ordered, Al atoms diffuse slowly. Thus, Al diffusion could not be as fast as that of Ni. It should be noted that we have not observed any intrasublattice jump of Al atoms through the Al sublattice ($\beta \leftrightarrow \beta$) in MD simulations.

From the above analysis, it is clear that the Ni vacancy plays an active role in both Ni and Al diffusion.

However, we have not observed the six-jump cycle mechanism in the MD simulation. This mechanism was proposed by Huntington [37]. In this model, diffusion occurs by a sequence

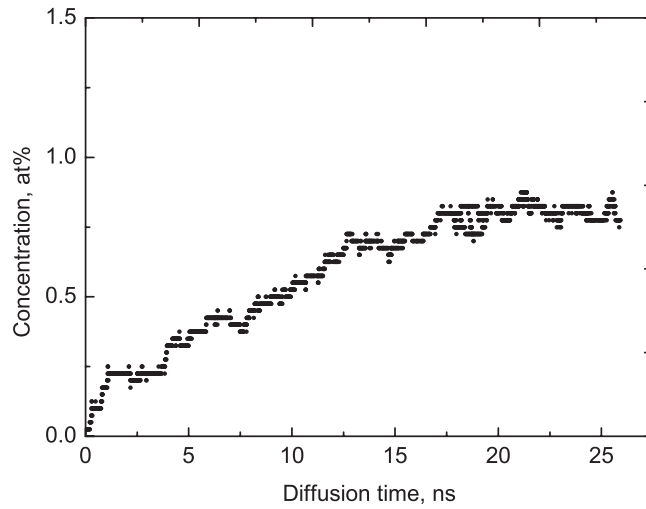


Figure 6. The concentration of Al antisites in Ni_3Al versus time at 1550 K.

Table 2. The Arrhenius parameters for diffusion of Ni in Ni_3Al .

Self-diffusion coefficient		Intra. mechanism		ASB mechanism	
D_0 ($\times 10^6 \text{ m}^2 \text{ s}^{-1}$)	E_m (eV)	Γ_0 ($\times 10^{14} \text{ s}^{-1}$)	E_m (eV)	Γ_0 ($\times 10^{16} \text{ s}^{-1}$)	E_m (eV)
9.17 ± 7.10	1.20 ± 0.10	8.80 ± 0.13	1.14 ± 0.18	1.93 ± 1.45	1.85 ± 0.10

of several individual jumps, so chosen that the final state has the same degree of order as the initial. Hancock [41] adapted this model to diffusion in Ni_3Al , and proposed two possible circuits, bent and straight, each consisting of six intersublattice jumps, as shown in figure 5.

The first three jumps of the cycle create three antisite defects; the next three restore order with the vacancy displaced. It is difficult to conclude that the six-jump cycle mechanism does not operate in Ni_3Al because of the limited time of the present MD simulation (35 ns). Moreover, the molecular simulation results are highly dependent on the interatomic potentials applied. To justify the MD simulation results and their potential dependence, I carried out MS simulations. The results are presented in section 3.2.

3.1.3. Temperature dependence of Ni diffusion coefficient. The Ni self-diffusion coefficient is calculated with equation (2) at each simulation temperature. The temperature dependence of the Ni self-diffusion coefficient D_{Ni}^* , together with the Ni vacancy diffusivity D_{Ni}^v , are plotted throughout the whole simulated temperature range, as shown in figure 7. These data cannot be fitted to the Arrhenius law with good accuracy. The parameters of Ni self-diffusion in Ni_3Al are summarized in table 2. The standard error of the pre-exponential factor of the Ni self-diffusion data is large. This could be explained in the following way. During the first 15 ns of simulation, the new antisite defects are created. Then the concentrations of antisite defects reach the dynamic equilibrium (see figure 6).

D_{Ni}^* is estimated over the whole simulation time using equation (2). This will result in a large uncertainty of value. As listed in table 2, the migration energy of Ni in Ni_3Al (1.20 ± 0.10 eV) is very close to the experimental value, 1.20 ± 0.2 eV [12]. The correlation factor for Ni diffusion determined with equation (3) is 0.64 ± 0.093 , which is very close

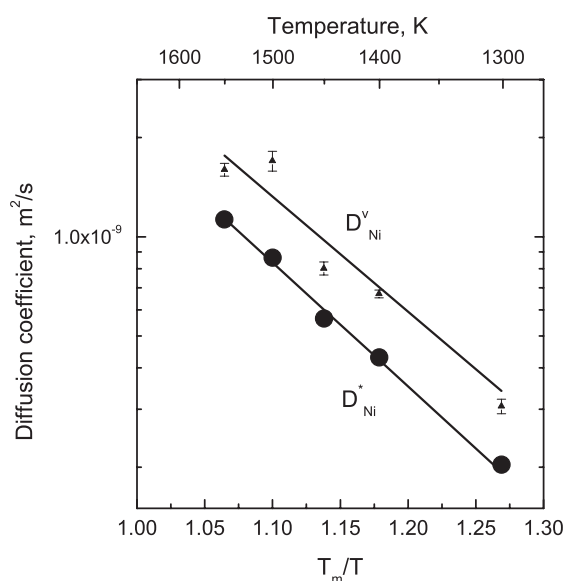


Figure 7. The MD simulation results of temperature dependence of the diffusion coefficient of Ni atoms and vacancy in Ni₃Al.

to the value of 0.688 calculated by Koiwa [14] assuming that Ni atoms diffuse only within Ni sublattices. This is consistent with the mechanism that Ni atoms migrate randomly via vacancies on the Ni sublattice.

It is difficult to observe Al diffusion when the temperature is below 1400 K. There are only three data points (1550, 1500 and 1450 K) available. They are very difficult to fit into the Arrhenius law with good accuracy, as shown in figure 8. The Al migration energy is roughly estimated to be 2.14 ± 0.97 eV. This is the first attempt to extract such information from MD simulations. We present these data for information. As defined before, the self-diffusion coefficients for both Ni and Al presented above are calculated per unit vacancy. The temperature and composition dependence of thermal vacancies and their effects on self-diffusion coefficients are not considered in the current study. Thus, direct quantitative comparison with experimental results should be made with caution. D_{Ni}^* estimated in the current study is an order of magnitude higher than D_{Al}^* . This result is consistent with the Al diffusion mechanism found in this simulation that Al atoms diffuse mainly by the intrasublattice and the ASB mechanism which are proportional to the concentrations of the Ni vacancy and the Al antisite. It seems to show the same qualitative trend as the results of Ikeda *et al* [15]. The reason for the difference between the results of Ikeda *et al* [15] and Fujiwara *et al* [18] is still not clear. As illustrated in figure 5, in the first 15 ns the Ni antisite defects have not reached the thermal equilibrium value. Thus, it is difficult to obtain enough Al atomic jumps whose possibility is proportional to the concentration of the Ni antisites. The current results, which are analysed based on trajectories (30 ns) twice as long as those in the preliminary results from the same simulations presented in [22], give better statistics on Ni and Al diffusion data, especially in the case of Al diffusion.

3.2. Molecular statics simulation of diffusion in Ni₃Al

The elementary jumps of both Ni and Al atoms in Ni₃Al, which are discussed in section 2.2, have been simulated with both FS and EAM interatomic potentials to obtain the migration

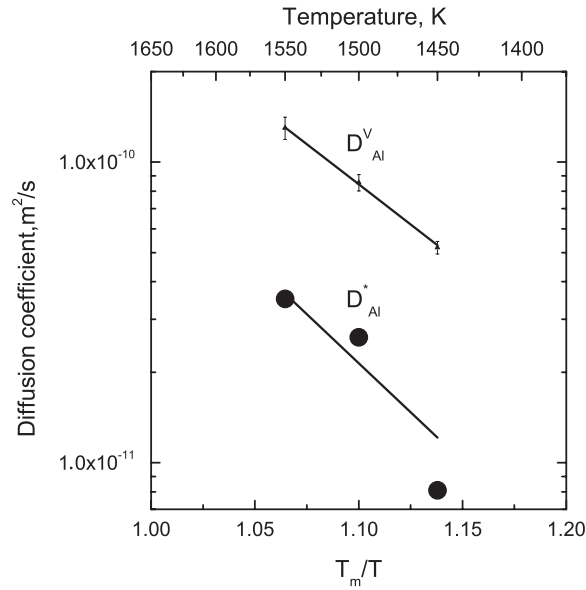


Figure 8. The MD simulation results of temperature dependence of the diffusion coefficient of Al atoms in Ni₃Al.

Table 3. The energy barriers of elementary jumps in Ni₃Al (eV).

Interatomic potentials	Interatomic potentials				
	$\omega_{\text{Ni}}^{\alpha\alpha}$	$\omega_{\text{Ni}}^{\alpha\beta}$	$\omega_{\text{Ni}}^{\beta\alpha}$	$\omega_{\text{Al}}^{\beta\alpha}$	$\omega_{\text{Al}}^{\alpha\alpha}$
FS	1.05	0.730	0.620	1.55	0.687
EAM	1.01	0.894	0.837	1.28	0.916

energies (E_m , eV) for these elementary jumps. The results are listed in table 3. The following discussions are based on the simulation results obtained from the FS interatomic potential. Ni atoms can diffuse through the Ni sublattice with the migration energy of 1.05 eV $\omega_{\text{Ni}}^{\alpha\alpha}$. However, a disordering jump ($\omega_{\text{Ni}}^{\alpha\beta}$, $E_m = 0.730$ eV) can be cancelled by the ordering jump ($\omega_{\text{Ni}}^{\beta\alpha}$, $E_m = 0.620$ eV). The jump of an Al atom to a Ni vacancy with the migration energy of 1.55 eV can be easily annealed by the reverse jump with the migration energy of only 0.250 eV. Although an Al_{Ni} once formed can readily migrate on the Ni sublattice ($\omega_{\text{Al}}^{\alpha\alpha}$) with the migration energy of 0.687 eV, its concentration is low (10^{-3} at.%, 1500 K) according to Sun [6] in highly ordered Ni₃Al. Thus, Al atoms seem to be difficult to diffuse. Schmidt *et al* [38] also calculated the elementary jumps by MS simulation. Belova *et al* [39] applied the results of Schmidt *et al* [38] in a kinetic Monte Carlo simulation of tracer diffusion [39] and the vacancy-wind factor [40], respectively. The results are consistent with those presented in the current research.

The simulations are carried out on the three diffusion mechanisms for Ni and Al diffusion (see table 4). The following results are presented in increasing order of activation energy.

The intrasublattice mechanism < the antistructure bridge mechanism < the six-jump cycle mechanism (straight) < the six-jump cycle mechanism (bent).

From these analyses (tables 3 and 4), it can be seen that these two types of interatomic potentials for Ni₃Al lead to the same trend of migration energies. The MS simulation results are summarized as follows. Ni atoms are predicated to diffuse through the Ni sublattice via

Table 4. The energy barriers of different diffusion mechanisms in Ni₃Al (eV).

Interatomic potentials	Intra. mech.	ASB		Six-jump cycle	
		Al	Ni	Straight	Bent
FS	0.684	1.14	0.63	2.23	2.70
EAM	0.921	1.09	0.837	1.74	2.25

the intrasublattice jump, which retains the order of the crystal. Diffusion of Al atoms in the perfect crystal starts with a disordering jump ($E_m = 1.55$ eV) of an Al atom from its home lattice to a Ni vacancy. So Al diffusion cannot occur in a simple way. The simulation of three types of multi-step diffusion mechanisms for Al diffusion in Ni₃Al shows that the intrasublattice mechanism and the antistructure bridge mechanism are energetically favourable while the six-jump cycle mechanism (both straight and bent) is less likely to occur because of the high migration energy (see table 4). The MD and MS simulations give the same results about diffusion mechanisms for both Ni and Al in Ni₃Al.

4. Conclusions

The diffusion mechanisms in order stoichiometric Ni₃Al are systematically studied using both MD and MS simulations. The results obtained from in this work are summarized as follows.

- (1) Both molecular statics and dynamics were applied to simulate diffusion in Ni₃Al. The results are at least qualitatively, and in some respect quantitatively, in agreement.
- (2) The simulations have revealed that Ni atoms mainly diffuse through the Ni sublattice via intrasublattice jumps. A Ni atom can also make antistructure jumps. These conclusions are consistent with experimental results and theoretical calculation. Diffusion of Al atoms is strongly temperature dependent, and at low temperature ($T < 1400$ K) Al atoms do not diffuse to a significant extent. When the temperature is above 1400 K, Al atoms diffuse via both the antistructure bridge and intrasublattice mechanisms. For highly ordered Ni₃Al, both mechanisms are Ni-antisite concentration dependent; Al diffusion is therefore limited.
- (3) The temperature dependence of the diffusion coefficient of Ni in Ni₃Al was estimated. The migration energy for Ni atoms is estimated to be 1.20 ± 0.10 eV. The correlation factor for Ni diffusion is 0.64 ± 0.0093 . The migration energy for Al atoms is estimated to be 2.14 ± 0.97 eV. The correlation factor for Al diffusion is 0.24 ± 0.08 .

Acknowledgments

I appreciate the members of the materials modelling group in Liverpool, UK, Dr Andrew F Calder for his help in organizing the computers, and Dr Alex Brasher and Dr Fei Gao (now at the Pacific North National Laboratory, US) for their help, encouragement and friendship during this research work. I wish to express special thanks to the University of Liverpool, UK, for offering me an international student fellowship and other financial support for this work.

References

- [1] Stoloff N S 1989 *Int. Mater. Rev.* **34** 153
- [2] Karnthaler H P, Muhlbacher E T and Rentenberger C 1996 *Acta Mater.* **44** 547
- [3] Czepe T and Wiezbinski S 2000 *Int. J. Mech. Sci.* **42** 1499
- [4] Frank S, Sodervall U and Herzig C 1995 *Phys. Status Solidi b* **191** 45
- [5] Badura-Gergen K and Schaefer H-E 1997 *Phys. Rev. B* **56** 3032

- [6] Sun J and Lin D 1994 *Acta Metall. Mater.* **42** 195
- [7] Gao F and Bacon D J 1993 *Phil. Mag.* A **67** 275
- [8] Gao F and Bacon D J 1993 *Phil. Mag.* A **67** 289
- [9] Hoshino K, Rothman S J and Averback R S 1988 *Acta Metall.* **36** 1271
- [10] Shi Y, Frohberg G and Wever H 1995 *Phys. Status Solidi a* **152** 361
- [11] Larikov L N, Grichenko V V and Flachenko V M 1984 *Diffusion Processes in Ordered Alloys* vol 14 (New Delhi: Amerind. Publ. Comp. Pvt. Ltd.) (translated for the Nat. Bur. Standards and Nat Sci. Found)
- [12] Wang T M, Shimotomai M and Doyama M 1984 *J. Phys. F: Met. Phys.* **14** 37
- [13] Divinski S V, Frank S, Sodervall U and Herzig C 1998 *Acta Mater.* **46** 4369
- [14] Koiwa M, Numakura H and Ishioka S 1997 *Defect Diffus. Forum* **143–147** 209
- [15] Ikeda T, Almazouzi A, Numakura H, Kowia M, Sprengel W and Nakajima H 1998 *Acta Mater.* **46** 5369
- [16] Manning J R 1961 *Phys. Rev.* **124** 470
- [17] Belova I and Murch G E 1998 *Phil. Mag.* A **78** 1085
- [18] Fujiwara K and Horita Z 2001 *Defect Diffus. Forum* **194–199** 565
- [19] Bakker H and Westerveld J P A 1988 *Phys. Status Solidi b* **145** 409
- [20] Debiaggi S B, Decorte P M and Monti A M 1996 *Phys. Status Solidi b* **195** 37
- [21] Athenes M and Bellon P 1999 *Phil. Mag.* A **79** 2242
- [22] Duan J, Osetsky Y N and Bacon D J 2001 *Defect Diffus. Forum* **194–199** 423
- [23] Daw M S and Baskes M I 1984 *Phys. Rev. B* **29** 6443
- [24] Finnis M W and Sinclair J E 1984 *Phil. Mag.* A **50** 45
- [25] Foiles S and Daw M S 1987 *J. Mater. Res.* **2** 5
- [26] Stocks G M, Pope D P and Giamei A F (ed) 1991 Alloy phase stability and design *Materials Research Society Symp. Proc. (San Francisco, CA)*
- [27] Caro A, Victoria M and Averback R S 1990 *J. Mater. Res.* **5** 1409
- [28] Gao F and Bacon D J 1995 *Phil. Mag.* A **71** 43
- [29] Gao F and Bacon D J 1995 *Phil. Mag.* A **71** 65
- [30] Gao F and Bacon D J 1997 *Phil. Mag.* A **75** 1603
- [31] Gao F and Bacon D J 2000 *Phil. Mag.* A **80** 1453
- [32] Manning J R 1971 *Phys. Rev. B* **4** 1111
- [33] Gunian M W, Stuart R N and Borg R J 1977 *Phys. Rev.* **15** 699
- [34] Mishin Y and Farkas D 1998 *Scr. Mater.* **39** 625
- [35] Evans D J and Morriss G P 1983 *Phys. Lett. A* **98** 433
- [36] Evans D J and Morriss G P 1983 *Chem. Phys.* **77** 63
- [37] Huntington H B, Miller N G and Nerses V 1961 *Acta Metall.* **9** 749
- [38] Schmidt C and Bocquet J 1998 *Mater. Res. Soc. Symp. Proc.* **527** 165
- [39] Belova I V and Murch G E 1999 *Defect Diffus. Forum* **177/178** 59
- [40] Belova I V and Murch G E 2001 *Defect Diffus. Forum* **194–199** 533
- [41] Hancock G F 1971 *Phys. Status Solidi a* **7** 535